

Self-assembly of zinc aminoporphyrins

Mark Gardner,^b Andrea J. Guerin,^a Christopher A. Hunter,^{*a} Ulrike Michelsen^a and Carmen Rotger[†]

^a Krebs Institute for Biomolecular Science, Department of Chemistry, University of Sheffield, Sheffield, UK S3 7HF

^b Discovery Chemistry, Pfizer Ltd, Sandwich, UK CT13 9NJ

Received (in Cambridge, UK) 9th October 1998, Accepted 4th November 1998

The aniline–zinc porphyrin interaction is an order of magnitude weaker than the corresponding pyridine–zinc porphyrin interaction, but it is still strong enough to cause self-assembly of zinc aminoporphyrins in solution. Three isomeric systems are reported, two form self-assembled dimers, but the geometry of the third forces it to form an open chain oligomer. The stabilities and structures of the complexes have been determined using ¹H NMR spectroscopy.

Introduction

Self-assembly is the spontaneous generation of well-defined molecular assemblies *via* non-covalent interactions, such as hydrogen-bonding and metal–ligand coordination.^{1–12} Porphyrins are popular building blocks because they are easily synthesized and functionalised, they are large and rigid, they are spectroscopically rich, and they have interesting photochemical and redox properties.^{13–16} We have been investigating the use of pyridine–zinc porphyrin coordination interactions for the self-assembly of oligomeric arrays of these chromophores.^{17–19} In the course of this work, we prepared a range of different aminoporphyrins, and when these compounds were metallated with zinc, they displayed some unusual spectroscopic properties. These are reported in this paper along with structural characterization of the complexes. We show that the aniline–zinc porphyrin coordination bond, although weaker than the pyridine–zinc porphyrin interaction,²⁰ is strong enough to yield stable self-assembled complexes.

Results and discussion

The three isomeric zinc aminoporphyrins, **2**, **3** and **4**, were all synthesised using the same procedure (Scheme 1).^{21,22} Starting from the appropriate nitrobenzaldehyde, a statistical reaction with pyrrole and *n*-pentylbenzaldehyde gave a mixture of porphyrin products. These were separated by column chromatography to give the mononitroporphyrin (H₂L⁶, H₂L⁷ or H₂L⁸) and the tetraalkylporphyrin (H₂L¹) which was used for control binding experiments. Each of the nitroporphyrins was reduced with stannous chloride and metallated with zinc acetate to give **2**, **3** and **4** in essentially quantitative yields. H₂L¹ was similarly metallated to give **1**.

The first evidence for the self-assembly of the three zinc aminoporphyrins came from the ¹H NMR spectra which were recorded at millimolar concentrations. The spectra were all concentration-dependent and surprisingly complex with many more signals than the corresponding free base porphyrins. At high concentrations, there were particularly large upfield shifts

for the signals due to the protons on the aniline ring which suggested that the lone pair of the aniline nitrogen of one porphyrin was coordinated to the vacant zinc binding site on the face of another porphyrin. This would bring the aniline into the shielding region of the coordinated porphyrin's ring current. To test this hypothesis, a ¹H NMR titration was carried out to measure the strength of the zinc–aniline interaction: a millimolar solution of **1** in *d*-chloroform was titrated with aliquots of a molar solution of L⁵. The association constant is 130 ± 10 M^{−1}, and the limiting complexation-induced changes in chemical shift are shown in Fig. 1. The aniline clearly coordinates to the zinc and lies over the face of the porphyrin.

The self-assembly properties of the three zinc aminoporphyrins were therefore investigated by quantitative ¹H NMR dilution experiments. The results for each system are discussed in turn.

Complex 2

At a concentration of 25 mM, the ¹H NMR spectrum of **2** was surprisingly complicated, and COSY and ROESY experiments were required to fully assign all of the signals. The complexity is caused by non-equivalence of the two faces of the porphyrin and slow rotation about all four *meso*-phenyl bonds

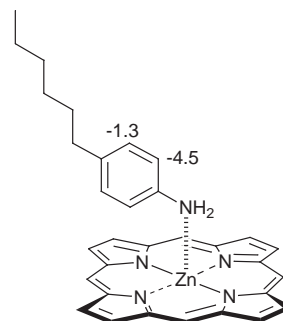
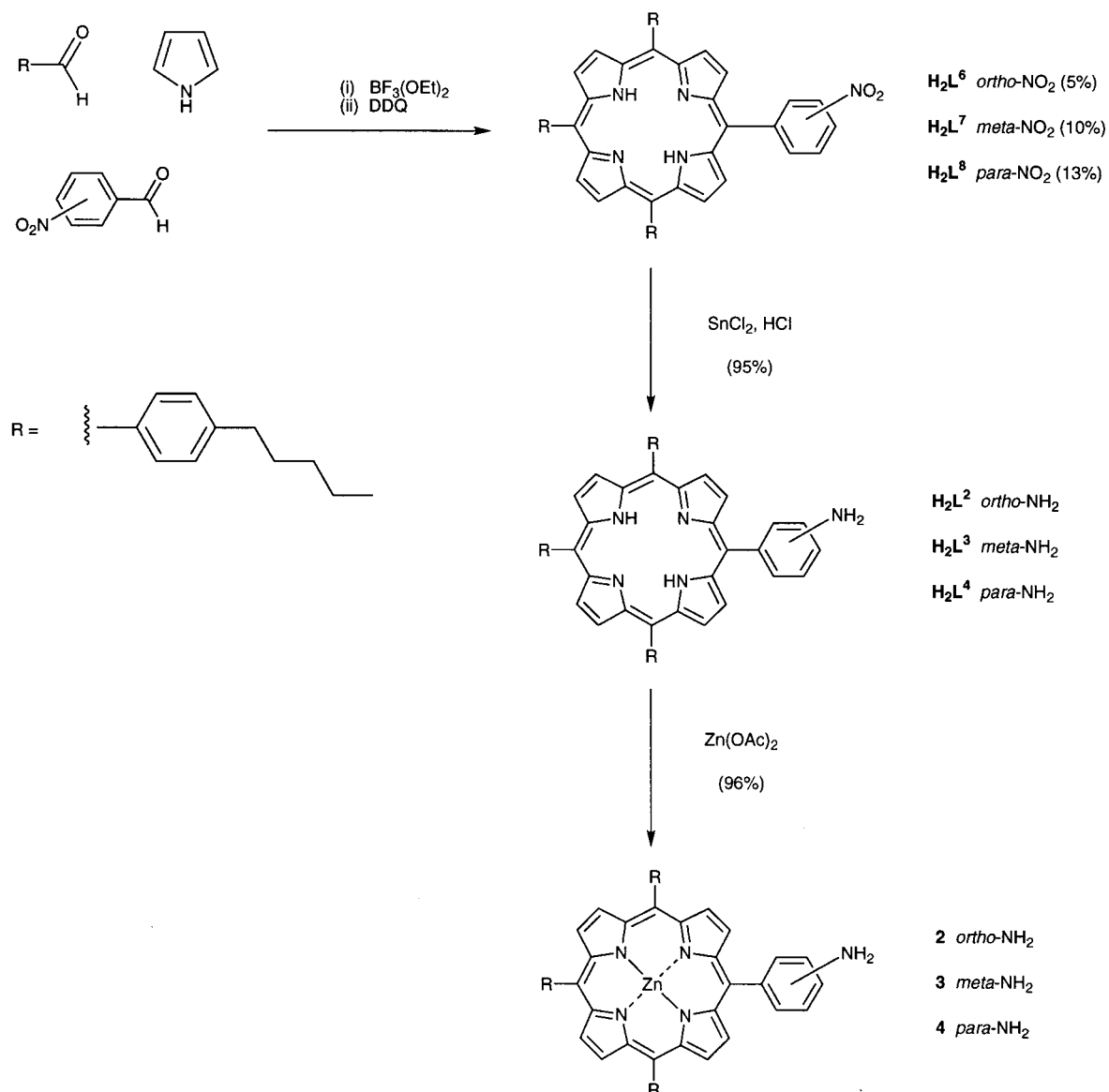


Fig. 1 Structure of the **1**·L⁵ complex, showing the limiting complexation-induced changes in chemical shift from the ¹H NMR titration in chloroform (some of the porphyrin *meso* substituents are omitted for clarity).

[†] Current address: Department of Chemistry, Universitat de les Illes Balears, 07071 Palma de Mallorca, Spain.



Scheme 1

on the NMR timescale. Clearly the rate of rotation about the *meso*-aniline bond is much slower than for the other three torsions due to the *ortho* substituent, but nevertheless on the NMR timescale, all are in slow exchange. In other systems such as H_2L^2 and H_2L^6 , this slow exchange has no impact on the appearance of the ^1H NMR spectrum, because there is very little difference between the environments on the two faces of the porphyrin. It is the self-assembly process that causes the difference between these two environments in **2**.

A detailed ^1H NMR dilution study was carried out on **2** in *d*-chloroform. The data could be fitted reasonably well to either a dimerisation isotherm or a non-cooperative linear polymerisation isotherm, but the dimer model was marginally better. The dimerisation constant is $160 \pm 20 \text{ M}^{-1}$ which is similar in magnitude to the value for the simple zinc-aniline interaction in $\mathbf{1} \cdot \text{L}^5$ and suggests that there is no cooperative self-assembly process in this system. However, this is not an appropriate comparison, because there is significant steric hindrance of the amine binding site in the *ortho*-derivative. In order to quantify this effect, we measured the $\mathbf{1} \cdot \text{H}_2\text{L}^2$ association constant (Fig. 2). It is difficult to obtain accurate values for the binding constant and complexation-induced changes in chemical shift for this complex, because it is very weakly bound, and it is therefore not possible to reach saturation in the binding isotherm. We estimate the association constant to

be $10 \pm 5 \text{ M}^{-1}$ which is significantly lower than the dimerisation constant for **2**. Thus **2** self-assembles *via* a cooperative process which suggests that the structure of the complex is a closed macrocyclic dimer held together by two zinc-aniline interactions (Fig. 3).²³ Of course, larger macrocyclic structures are also consistent with this data, but a dimer is entropically favoured, and this structure is supported by the chemical shift data discussed below.

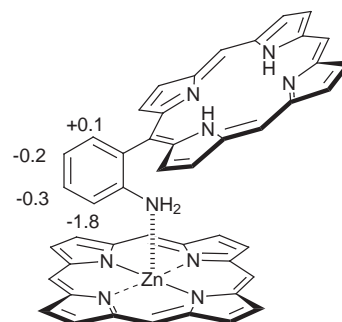
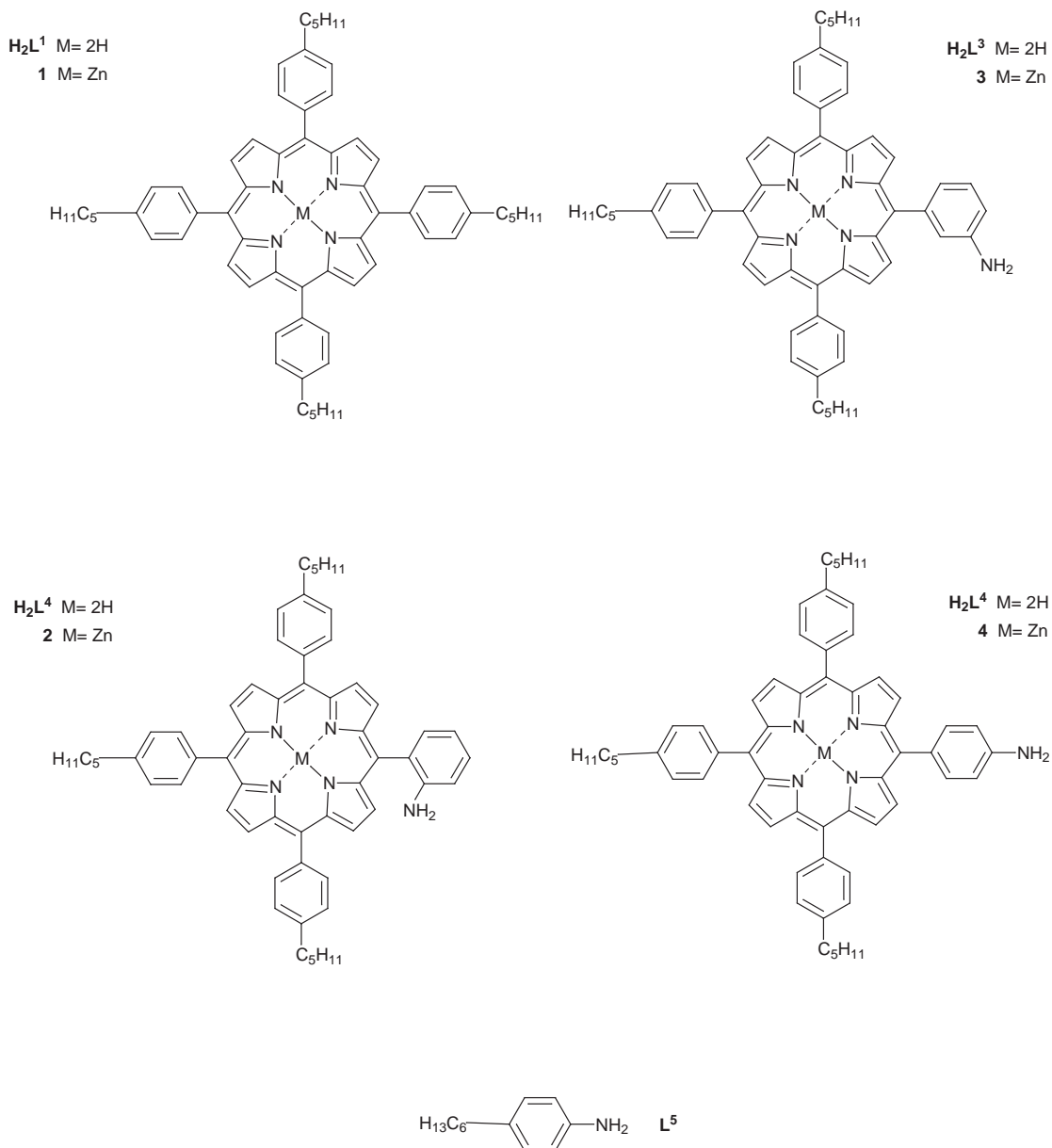


Fig. 2 Structure of the $\mathbf{1} \cdot \text{H}_2\text{L}^2$ complex, showing the limiting complexation-induced changes in chemical shift from the ^1H NMR titration in chloroform (some of the porphyrin *meso* substituents are omitted for clarity).



The limiting complexation-induced changes in chemical shift (CIS) for $1 \cdot H_2L^2$ and $(2)_2$ are shown in Fig. 2 and 3 respectively. Although the magnitudes of the values for $1 \cdot H_2L^2$ are subject to a large error due to the low stability of the complex, the pattern of shift changes is accurate and is quite different from that found for $(2)_2$ indicating that the anilines are bound in different orientations in the two systems. Very large changes in chemical shift are found for the porphyrin β -pyrrole signals as well as the signals due to the protons on the aniline ring. CIS values can be used in a quantitative manner to obtain more detailed information about the structures of porphyrin complexes of this type.^{24–26} We have recently developed a computational method for deriving high resolution three-dimensional structural information on supramolecular complexes from complexation-induced changes in chemical shift,²⁷ and this was used to obtain the three-dimensional structure of $(2)_2$ which is shown in Fig. 4 (see Experimental section for details). The CIS values for the optimised dimer structure agree extremely well with the experimental data: root mean square difference (rmsd) = 0.03 ppm.

Complex 3

Like **2**, the 1H NMR spectrum of **3** was surprisingly complicated at high concentrations, and COSY and ROESY experi-

ments were required to fully assign the spectrum. The two faces of the porphyrin are again different, and rotation about the *meso*-phenyl bonds is slow on the NMR timescale. The low concentration spectrum and the spectra of the corresponding free base porphyrins H_2L^3 and H_2L^7 are relatively simple which implies that it is the self-assembly process which causes the two faces of the porphyrin to become non-equivalent. A 1H NMR dilution study was carried out in *d*-chloroform. The data could be fitted equally well to either a dimerisation isotherm or a non-cooperative linear polymerisation isotherm, but the association constants are an order of magnitude larger than the value for the simple zinc-aniline interaction in $1 \cdot L^5$ (the association constant for dimerisation is $1080 \pm 90 M^{-1}$). This implies that formation of the complex is a cooperative process involving more than one coordination bond, *i.e.* the complex is a closed macrocycle held together by two zinc-aniline interactions per monomer. Entropically, the most favourable structure is a dimer (Fig. 5), and this is supported by the CIS data discussed below.

The limiting complexation-induced changes in chemical shift for $(3)_2$ are shown in Fig. 5. The pattern of shift changes is similar to that found for **2** except that the values for the porphyrin β -pyrrole signals are significantly smaller. These CIS values were used in conjunction with the computational method discussed above to obtain a three-dimensional struc-

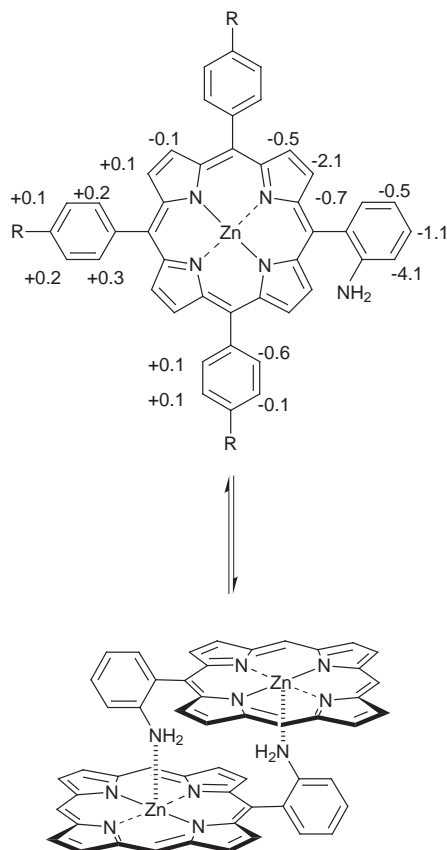


Fig. 3 Limiting complexation-induced changes in chemical shift from the ¹H NMR dilution of **2** (the signals due to the anilino protons were difficult to identify reliably and reproducibly). The structure of the self-assembled dimer is also shown. Some of the porphyrin *meso* substituents are omitted for clarity.

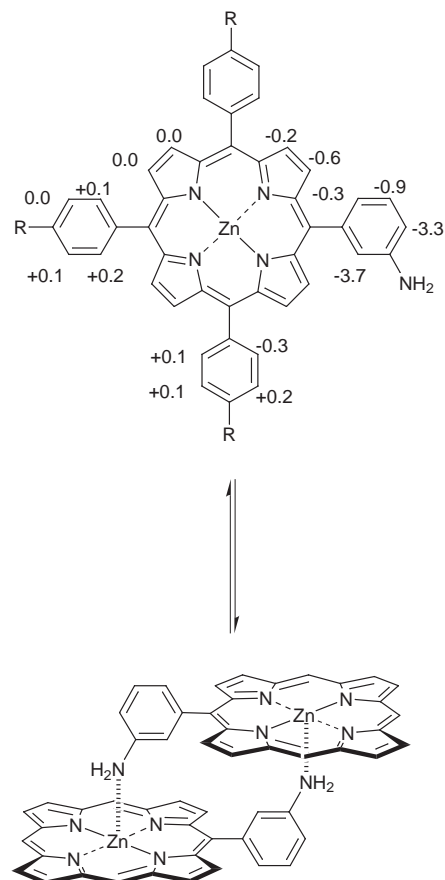


Fig. 5 Limiting complexation-induced changes in chemical shift from the ¹H NMR dilution of **3** (the signals due to the anilino protons were difficult to identify reliably and reproducibly). The structure of the self-assembled dimer is also shown. Some of the porphyrin *meso* substituents are omitted for clarity.

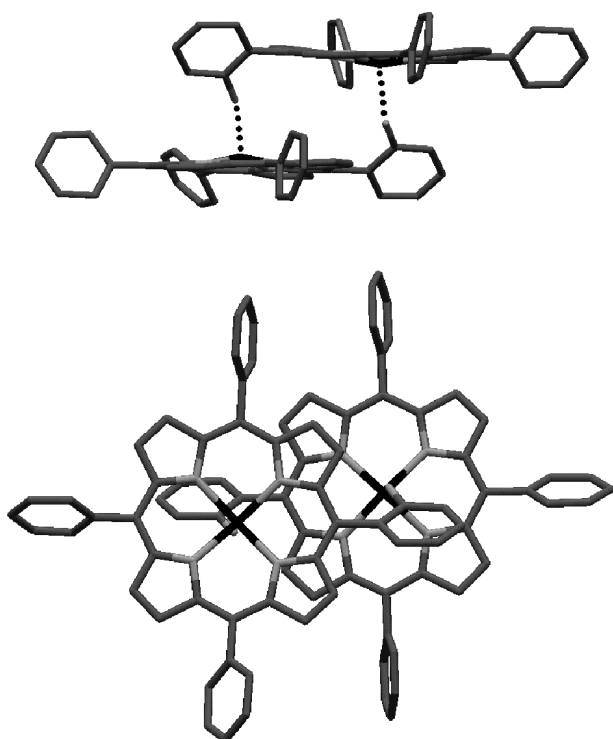


Fig. 4 Two views of the three-dimensional structure of the self-assembled dimer (2)₂. The structure was determined by matching calculated complexation-induced changes in ¹H NMR chemical shift with the experimental values.

ture (Fig. 6). The calculated CIS values for the optimised dimer structure agree extremely well with the experimental data: rmsd = 0.02 ppm. The reason for the difference in the pattern of chemical shift changes for **2** and **3** can easily be seen by comparing the structures in Fig. 4 and 6: in **2**, the β -pyrrole protons on the edge of one porphyrin lie over the centre of the ring current of the neighbouring molecule, but moving the substituent from the *ortho* to the *meta* position increases the lateral displacement of the porphyrin rings and significantly reduces the extent of overlap.

Complex 4

The behaviour of **4** was quite different from the other two systems. All of the signals in the ¹H NMR spectrum of **4** were broad at a concentration of 25 mM but became much sharper at lower concentrations. The line-broadening suggests that self-assembly generates a high molecular weight oligomeric species (a chemical exchange process is an alternative explanation). A ¹H NMR dilution study was carried out in *d*-chloroform. The data could be fitted equally well to either a dimerisation isotherm or a non-cooperative linear oligomerisation isotherm, but the association constants are very similar to the value for the simple zinc-aniline interaction in 1·L⁵ (the association constant for open chain oligomerisation is $190 \pm 20 \text{ M}^{-1}$). This implies that there are no cooperative processes in this system and suggests that an open linear oligomer is the most likely structure of the complex (Fig. 7).²³ The limiting complexation-induced changes in chemical shift are shown in Fig. 7. The values for the aniline ring protons are comparable with those found for the 1·L⁵ complex (Fig. 1)

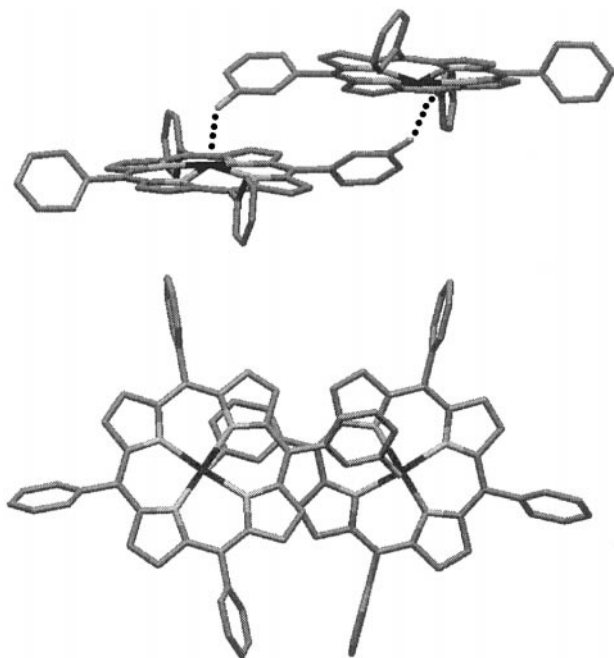


Fig. 6 Two views of the three-dimensional structure of the self-assembled dimer (3)₂. The structure was determined by matching calculated complexation-induced changes in ^1H NMR chemical shift with the experimental values.

indicating that the aniline is bound in a similar orientation in both systems. The pattern of shifts on the porphyrin ring are similar to **3**, but the *meso* substituents experience much larger ring current-induced upfield shifts. This suggests a more

upright structure for this complex with the 10- and 20-*meso* substituents lying over the ring current of the neighbouring molecule. Attempts to use the CIS values to determine the three-dimensional structure of a closed dimer failed for this system: the conformational search was unable to locate a compatible dimeric structure. Thus the CIS data also support formation of a simple oligomeric aggregate for **4**. This behaviour can easily be rationalised on the basis of the geometry of the system: it is not sterically possible to form a closed dimeric complex with the *para*-substituent.

Further evidence for the structures of the assemblies was sought from mass spectrometry and vapor pressure osmometry, but the complexes are not sufficiently stable to be characterized using these techniques. Similarly, self-assembly does not take place at concentrations suitable for UV/Visible absorption spectroscopy.

Conclusions

The stability constant for coordination of a zinc porphyrin by aniline is approximately 100 M^{-1} . This is one order of magnitude weaker than the stability of pyridine–zinc porphyrin complexes. Nevertheless stable oligomeric assemblies of zinc aminoporphyrins are formed in solution. The *ortho* and *meta* zinc amino porphyrin derivatives, **2** and **3**, form closed dimers with significant cooperativity between the two zinc–nitrogen bonds which hold the macrocycle together. The geometry of the *para* derivative precludes the formation of macrocyclic dimers, and so this compound forms an open chain linear oligomer with no cooperativity. The large ring current shifts in the ^1H NMR spectra provide detailed information about the three-dimensional structures of the complexes and have been used to derive high resolution structures of the two dimers.

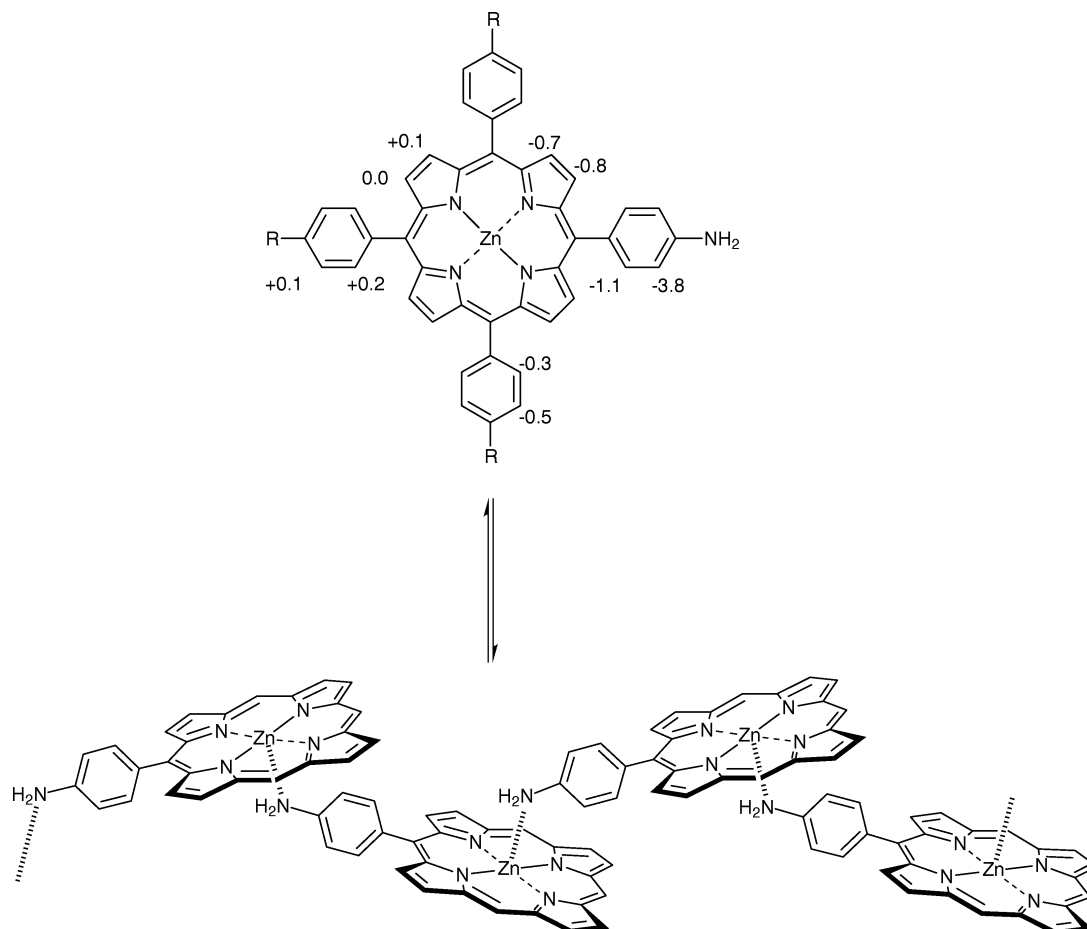


Fig. 7 Limiting complexation-induced changes in chemical shift from the ^1H NMR dilution of **4** (the signals due to the anilino protons were difficult to identify reliably and reproducibly). The structure of the self-assembled oligomeric chain is also shown. Some of the porphyrin *meso* substituents are omitted for clarity.

Experimental

¹H NMR dilution experiments

A sample of known concentration (of the order 10–100 mM) in CDCl₃ was prepared and a ¹H NMR spectrum was recorded on a 0.8 ml sample. From this sample, 0.4 ml was removed and replaced by 0.4 ml of solvent. After shaking to mix the solvents, a second ¹H NMR spectrum was recorded. This procedure was repeated until there was no further change in chemical shift or the sample was too dilute to record a spectrum. For signals that moved more than 0.01 ppm over the whole concentration range, the chemical shifts at each concentration were recorded and fitted to a dimerisation or non-cooperative linear polymerisation isotherm using purpose written software on an Apple Macintosh microcomputer, *NMRDil_Dimer* or *NMRDil_Agg*. These programs use a Simplex procedure to fit the experimental data to the following equations to determine the optimum solutions for the association constant, and the limiting bound and free chemical shifts.

NMRDil_Dimer fits the data to a dimerisation isotherm by solving the following equations:

$$[AA] = \frac{1 + 4K_d[A]_0 - \sqrt{\{1 + 8K_d[A]_0\}}}{8K_d} \quad (1)$$

$$[A] = [A]_0 - 2[AA] \quad (2)$$

$$\delta_{\text{obs}} = \frac{2[AA]}{[A]_0} \delta_d + \frac{[A]}{[A]_0} \delta_f \quad (3)$$

where $[A]_0$ is the total concentration, $[A]$ is the concentration of unbound free species, $[AA]$ is the concentration of dimer, K_d is the dimerisation constant, δ_f is the free chemical shift, and δ_d is the limiting bound chemical shift of the dimer.

NMRDil_Agg fits the data to a non-cooperative linear oligomerisation/polymerisation isotherm by solving the following equations:

$$[Agg] = [A]_0 \left\{ 1 - \frac{2}{1 + \sqrt{\{1 + 4K[A]_0\}}} \right\} \quad (4)$$

$$[A] = [A]_0 - [Agg] \quad (5)$$

$$\delta_{\text{obs}} = \frac{2[Agg]}{[A]_0} \delta_b + \frac{[A]}{[A]_0} \delta_f \quad (6)$$

where $[A]_0$ is the total concentration, $[A]$ is the concentration of sites which are unbound (this is the sum of the free species and the ends of the aggregate which are not bound), $[Agg]$ is the concentration of sites involved in intermolecular interactions in the aggregate, K is the association constant for chain extension of the aggregate, δ_f is the free chemical shift, and δ_b is the limiting bound chemical shift of the bound sites in the aggregate.

Several signals were followed in each experiment, and the value quoted for the association constant is the weighted average based on the observed changes in chemical shift. The errors quoted are twice the standard error (95% confidence limit).

Complexation-induced change in chemical shift calculations

The method used to determine three-dimensional structures from complexation-induced changes in chemical shift has been described in detail elsewhere.²⁷ In this work, the porphyrin ring current shifts were calculated using the eight loop Haigh–Mallion model developed by Cross and Wright with ring current intensity factors of 1.99 for the six-membered rings and 0.55 for the five-membered rings.²⁸

The conformational searches were carried out using the same protocol for each system. The structures of the zinc porphyrins were taken from the X-ray crystal structure analysis of the pyridine complex of zinc tetraphenylporphyrin, and amine groups were added using standard bond lengths and angles in Macromodel.²⁹ A genetic algorithm was used to optimise the conformation of the complex so that the calculated CIS values matched the experimental values as closely as possible. We allowed intermolecular translation (± 10 Å) and rotation ($\pm 180^\circ$) as well as intramolecular torsional changes ($\pm 180^\circ$) for all four *meso*-phenyl bonds in each molecule. To restrict the search space, the amine nitrogens were constrained to be within 2.1 ± 0.5 Å of the zinc atoms, and van der Waals clashes were penalised at distances of less than 3 Å for intermolecular clashes and 2 Å for intramolecular clashes for non-hydrogen atoms. The searches for both **2** and **3** converged to values of $R_{\text{expt}}/R_{\Delta\delta}$ of 9.0 and 13.5 respectively in about 2000 generations for a population of 100 (R_{expt} is the rms of the experimentally observed CIS values, and $R_{\Delta\delta}$ is the rms difference between the calculated and experimental values). The **4** search failed to converge to a satisfactory solution: the maximum $R_{\text{expt}}/R_{\Delta\delta}$ value reached was 1.9.

Preparation of porphyrins

Freshly distilled pyrrole (1.39 ml, 0.02 mol, 1 equivalent), the appropriate nitrobenzaldehyde (1.207 g, 0.008 mol, 0.4 equivalent), 4-*n*-pentylbenzaldehyde (2.112 g, 0.012 mol, 0.6 equivalent), dry EtOH (13 ml) and dry dichloromethane (2 l) were stirred under N₂ for 5 min. BF₃·OEt₂ (1 ml, 6.6 mmol, 0.33 equivalent) was added *via* a septum, and the reaction mixture was protected from light and stirred under nitrogen for 70 min. 2,3-Dicyano-5,6-dichloro-1,4-benzoquinone (DDQ) (4.54 g, 0.02 mol, 1 equivalent) was added, and the reaction mixture was stirred for a further 90 min before the addition of triethylamine (2.8 ml). The solvent was removed *in vacuo*, and the black residue was washed with methanol in a Soxhlet to remove polymeric material. The solid residue was dissolved in dichloromethane and passed through a short plug of Florisil eluting with light petroleum–CHCl₃ (1 : 1, bp range for light petroleum; 40–60 °C) to remove any remaining polymer. The solvent was removed *in vacuo*, and the porphyrin products were separated by column chromatography on silica eluting with light petroleum–CHCl₃ (2 : 1). The first band was H₂L¹ which was recrystallised from CHCl₃–CH₃OH to give purple plates (0.3–0.8 g, 8–16%). The second band was the mononitroporphyrin which was recrystallised in the same manner to give a dark purple powder.

5,10,15,20 - Tetrakis(4 - pentylphenyl) - 21H,23H - porphine H₂L¹. Mp 313–316 °C (Found: C, 85.66; H, 7.88; N, 6.24. Calc. for C₆₄H₇₀N₄: C, 85.86; H, 7.88; N, 6.26%); λ_{max} (CH₂Cl₂)/nm 420 ($\epsilon/\text{dm}^3 \text{ mol}^{-1}$ 530 000), 517 (25 000), 551 (16 000) and 598 (9 300); δ_{H} (CDCl₃) 8.87 (8H, s, β -pyrrolic H), 8.12 (8H, d, *J* 7, ArH_o), 7.56 (8H, d, *J* 7, ArH_m), 2.96 (8H, t, *J* 7, ArCH₂), 1.93 (8H, qn, *J* 7, CH₂), 1.52 (16H, m, 8 × CH₂), 1.03 (12H, t, *J* 7 Hz, CH₃), –2.75 (2H, s, NH); *m/z* (FAB) 895 (M⁺, C₆₄H₇₀N₄ requires 895.2962).

5 - (2-Nitrophenyl) - 10,15,20 - tris(4 - pentylphenyl) - 21H,23H - porphine H₂L⁶. Yield 0.44 g, 10%; mp 199–201 °C; λ_{max} (CH₂Cl₂)/nm 423 ($\epsilon/\text{dm}^3 \text{ mol}^{-1}$ 640 000), 518 (13 400), 554 (6 810), 593 (3 990) and 649 (3 070); δ_{H} (CDCl₃) 8.88 (2H, d, *J* 7, β -pyrrolic H), 8.86 (4H, s, β -pyrrolic H), 8.64 (2H, d, *J* 7, β -pyrrolic H), 8.45 (1H, d, *J* 7, 5-H₆), 8.24 (1H, d, *J* 7, 5-H₃), 8.10 (6H, m, 10-, 15- and 20-H_o), 7.95 (2H, m, 5-H₄ and 5-H₅), 7.50 (6H, d, *J* 7, 10-, 15- and 20-H_m), 2.94 (6H, t, *J* 7, ArCH₂), 1.95 (6H, qn, *J* 7, CH₂), 1.50 (12H, m, 6 × CH₂), 1.05 (9H, t, *J* 7 Hz, CH₃), –2.72 (2H, s, NH); *m/z* (FAB) 870 (M⁺, C₅₉H₅₉N₅O₂ requires 870.1793).

5-(3-Nitrophenyl)-10,15,20-tris(4-pentylphenyl)-21H,23H-porphine H_2L^7 . Yield 0.22 g, 5%; mp 259–261 °C; λ_{\max} (CH_2Cl_2)/nm 421 ($\epsilon/dm^3 \text{ mol}^{-1} \text{ cm}^{-1}$ 360 000), 518 (19 000), 554 (9 590), 592 (5 890) and 648 (4 710); $\delta_H(CDCl_3)$ 9.10 (1H, s, 5-H₂), 8.92 (2H, d, *J* 7, β -pyrrolic H), 8.87 (4H, s, β -pyrrolic H), 8.70 (2H, d, *J* 7, β -pyrrolic H), 8.68 (1H, d, *J* 7, 5-H₄), 8.58 (1H, d, *J* 7, 5-H₆), 8.15 (6H, m, 10-, 15- and 20-H_o), 7.95 (1H, t, *J* 7, 5-H₅), 7.60 (6H, d, *J* 7, 10-, 15- and 20-H_m), 2.97 (6H, t, *J* 7, ArCH₂), 1.94 (6H, qn, *J* 7, CH₂), 1.50 (12H, m, 6 \times CH₂), 1.05 (9H, t, *J* 7 Hz, CH₃), –2.75 (2H, s, NH); *m/z* (FAB) 870 (M^+ , $C_{59}H_{59}N_5O_2$ requires 870.1793).

5-(4-Nitrophenyl)-10,15,20-tris(4-pentylphenyl)-21H,23H-porphine H_2L^4 . Yield 0.56 g, 13%; mp 243–245 °C; λ_{\max} (CH_2Cl_2)/nm 421 ($\epsilon/dm^3 \text{ mol}^{-1} \text{ cm}^{-1}$ 330 000), 518 (18 000), 554 (11 000), 593 (6 500) and 649 (5 300); $\delta_H(CDCl_3)$ 8.92 (2H, d, *J* 7, β -pyrrolic H), 8.88 (4H, s, β -pyrrolic H), 8.73 (2H, d, *J* 7, β -pyrrolic H), 8.63 (2H, d, *J* 7, 5-H₂ and 5-H₆), 8.40 (2H, d, *J* 7, 5-H₃ and 5-H₅), 8.12 (6H, d, *J* 7, 10-, 15- and 20-H_o), 7.56 (6H, d, *J* 7, 10-, 15- and 20-H_m), 2.96 (6H, t, *J* 7, ArCH₂), 1.93 (6H, qn, *J* 7, CH₂), 1.54 (12H, m, 6 \times CH₂), 1.05 (9H, t, *J* 7 Hz, CH₃), –2.75 (2H, s, NH); *m/z* (FAB) 870 (M^+ , $C_{59}H_{59}N_5O_2$ requires 870.1793).

General procedure for reduction of nitroporphyrins

The mononitroporphyrin (200 mg, 0.230 mmol, 1 equivalent) was dissolved in 1,4-dioxane (45 cm³). SnCl₂ · 2H₂O (600 mg, 2.66 mmol, 12 equivalents) and concentrated HCl (70 cm³) were added. The reaction vessel was protected from light and heated for 60 min under argon using a preheated oil bath (70 °C). After removing the heat source, the hot reaction mixture was basified by adding concentrated NH₃ and then allowed to cool to room temperature. The product was extracted with ethyl acetate (3 \times 50 cm³). The organic fractions were combined, washed with water, dried over Na₂SO₄ and filtered. The solvent was removed *in vacuo*, and the product was purified by column chromatography on silica eluting with light petroleum–CH₂Cl₂ (1 : 4). The product was recrystallised from CH₂Cl₂–CH₃OH giving a purple powder (0.18 g, 95%).

5-(2-Aminophenyl)-10,15,20-tris(4-pentylphenyl)-21H,23H-porphine H_2L^2 . Mp 169–171 °C; λ_{\max} (cyclohexane)/nm 423 ($\epsilon/dm^3 \text{ mol}^{-1} \text{ cm}^{-1}$ 94 500), 517 (19 200), 553 (9 240), 592 (5 550) and 647 (4 540); $\delta_H(CDCl_3)$ 8.80 (8H, s, β -pyrrolic H), 8.05 (6H, m, 10-, 15- and 20-H_o), 7.84 (1H, d, *J* 7, 5-H₆), 7.53 (1H, t, *J* 7, 5-H₄), 7.50 (6H, d, *J* 7, 10-, 15- and 20-H_m), 7.25 (1H, t, *J* 7, 5-H₅), 7.10 (1H, d, *J* 7, 5-H₃), 3.50 (2H, s, NH₂), 2.94 (6H, t, *J* 7, ArCH₂), 1.95 (6H, qn, *J* 7, CH₂), 1.50 (12H, m, 6 \times CH₂), 1.05 (9H, t, *J* 7 Hz, CH₃), –2.80 (2H, s, NH); *m/z* (FAB) 840 (M^+ , $C_{59}H_{61}N_5$ requires 840.1644).

5-(3-Aminophenyl)-10,15,20-tris(4-pentylphenyl)-21H,23H-porphine H_2L^3 . Mp 153–155 °C; λ_{\max} (CH_2Cl_2)/nm 421 ($\epsilon/dm^3 \text{ mol}^{-1} \text{ cm}^{-1}$ 328 000), 517 (13 000), 552 (6 890), 593 (3 840) and 648 (3 500); $\delta_H(CDCl_3)$ 8.93 (2H, d, *J* 7, β -pyrrolic H), 8.84 (4H, s, β -pyrrolic H), 8.82 (2H, d, *J* 7, β -pyrrolic H), 8.10 (6H, d, *J* 7, 10-, 15- and 20-H_o), 7.62 (1H, t, *J* 7, 5-H₆), 7.50 (7H, m, 10-, 15- and 20-H_m and 5-H₂), 7.47 (1H, d, *J* 7, 5-H₅), 7.10 (1H, d, *J* 7, 5-H₄), 3.94 (2H, s, NH₂), 2.94 (6H, t, *J* 7, ArCH₂), 1.95 (6H, qn, *J* 7, CH₂), 1.50 (12H, m, 6 \times CH₂), 1.05 (9H, t, *J* 7 Hz, CH₃), –2.80 (2H, s, NH); *m/z* (FAB) 841 (M^+ , $C_{59}H_{61}N_5$ requires 840.1644).

5-(4-Aminophenyl)-10,15,20-tris(4-pentylphenyl)-21H,23H-porphine H_2L^4 . Mp 147–149 °C; λ_{\max} (CH_2Cl_2)/nm 422 ($\epsilon/dm^3 \text{ mol}^{-1} \text{ cm}^{-1}$ 290 000), 519 (15 000), 557 (10 000), 594 (4 600) and 650 (5 300); $\delta_H(CDCl_3)$ 8.91 (4H, m, β -pyrrolic H), 8.87 (4H, s, β -pyrrolic H), 8.10 (6H, d, *J* 7, 10-, 15- and 20-H_o), 8.00

(2H, d, *J* 7, 5-H₂ and 5-H₆), 7.55 (6H, d, *J* 7, 10-, 15- and 20-H_m), 7.10 (2H, d, *J* 7, 5-H₃ and 5-H₅), 4.05 (2H, s, NH₂), 2.95 (6H, t, *J* 7, ArCH₂), 1.90 (6H, qn, *J* 7, CH₂), 1.4–1.6 (12H, m, 6 \times CH₂), 1.05 (9H, t, *J* 7 Hz, CH₃), –2.75 (2H, s, NH); *m/z* (FAB) 840 (M^+ , $C_{59}H_{61}N_5$ requires 840.1644).

General procedure for the metallation of porphyrins

The free base porphyrin (36 mg, 0.04 mmol, 1 equivalent) was dissolved in CH₂Cl₂–CH₃OH (3 : 1, 30 ml) and zinc acetate (94 mg, 0.4 mmol, 10 equivalents) was added. The reaction mixture was protected from light and stirred at room temperature for 60 min. The solvent was removed *in vacuo*, and the product was purified by column chromatography on basic alumina eluting with CH₂Cl₂–CH₃OH (99 : 1). Recrystallisation from CHCl₃–CH₃OH yielded the product as a purple powder (37 mg, 96%).

[5,10,15,20-Tetrakis(4-pentylphenyl)-21H,23H-porphinato]-zinc 1. Mp 309–311 °C (Found: C, 80.23; H, 7.25; N, 5.87. Calc. for $C_{64}H_{68}N_4Zn$: C, 80.19; H, 7.15; N, 6.26%); λ_{\max} (CH_2Cl_2)/nm 422 ($\epsilon/dm^3 \text{ mol}^{-1} \text{ cm}^{-1}$ 650 000), 551 (26 000) and 592 (8 300); $\delta_H(CDCl_3)$ 8.98 (8H, s, β -pyrrolic H), 8.12 (8H, d, *J* 7, ArH_o), 7.55 (8H, d, *J* 7, ArH_m), 2.96 (8H, t, *J* 7, ArCH₂), 1.93 (8H, qn, *J* 7, CH₂), 1.52 (16H, m, 8 \times CH₂), 1.03 (12H, t, *J* 7 Hz, CH₃); *m/z* (FAB) 957 (M^+ , $C_{64}H_{68}N_4Zn$ requires 957.51).

[5-(2-Aminophenyl)-10,15,20-(4-pentylphenyl)-21H,23H-porphinato]zinc 2. Mp 227–230 °C; λ_{\max} (CH_2Cl_2)/nm 423 ($\epsilon/dm^3 \text{ mol}^{-1} \text{ cm}^{-1}$ 61 500), 549 (29 100) and 589 (6 760); $\delta_H(CDCl_3)$ concentration-dependent, 9.04 (2H, d, *J* 7, β -pyrrolic H), 8.92 (2H, d, *J* 7, β -pyrrolic H), 8.70 (2H, d, *J* 7, β -pyrrolic H), 8.28 (1H, d, *J* 7, 15-H_o), 8.20 (1H, d, *J* 7, 15-H_o), 8.17 (2H, d, *J* 7, 10- and 20-H_o), 8.08 (2H, d, *J* 7, β -pyrrolic H), 7.93 (2H, d, *J* 7, 10- and 20-H_o), 7.75 (1H, d, *J* 7, 15-H_m), 7.60 (1H, d, *J* 7, 15-H_m), 7.60 (2H, d, *J* 7, 10- and 20-H_m), 7.48 (2H, d, *J* 7, 10- and 20-H_m), 7.48 (1H, d, *J* 7, 5-H₆), 7.08 (1H, t, *J* 7, 5-H₄), 6.94 (1H, t, *J* 7, 5-H₅), 4.91 (1H, d, *J* 7, 5-H₃), 2.85 (6H, t, *J* 7, ArCH₂), 1.88 (6H, qn, *J* 7, CH₂), 1.48 (12H, m, 6 \times CH₂), 1.00 (9H, t, *J* 7 Hz, CH₃), 0.60 (2H, s, NH₂); *m/z* (FAB) 903 (M^+ , $C_{59}H_{59}N_5Zn$ requires 903.4886).

[5-(3-Aminophenyl)-10,15,20-(4-pentylphenyl)-21H,23H-porphinato]zinc 3. Mp 169–172 °C; λ_{\max} ($CHCl_3$)/nm 422 ($\epsilon/dm^3 \text{ mol}^{-1} \text{ cm}^{-1}$ 307 000), 549 (14 600) and 589 (2 940); $\delta_H(CDCl_3)$ concentration-dependent, 9.03 (2H, d, *J* 7, β -pyrrolic H), 8.95 (2H, d, *J* 7, β -pyrrolic H), 8.71 (2H, d, *J* 7, β -pyrrolic H), 8.25 (2H, m, β -pyrrolic H), 8.29 (2H, d, *J* 7, 10- and 20-H_o), 8.20 (1H, d, *J* 7, 15-H_o), 8.16 (1H, d, *J* 7, 15-H_o), 7.94 (2H, d, *J* 7, 10- and 20-H_o), 7.69 (1H, d, *J* 7, 15-H_m), 7.62 (2H, d, *J* 7, 10- and 20-H_m), 7.57 (1H, d, *J* 7, 15-H_m), 7.46 (2H, d, *J* 7, 10- and 20-H_m), 7.32 (1H, d, *J* 7, 5-H₆), 6.62 (1H, t, *J* 7, 5-H₅), 3.83 (2H, m, 5-H₂ and 5-H₄), 2.96 (6H, t, *J* 7, ArCH₂), 1.94 (6H, qn, *J* 7, CH₂), 1.50 (12H, m, 6 \times CH₂), 1.04 (9H, t, *J* 7 Hz, CH₃); *m/z* (FAB) 903 (M^+ , $C_{59}H_{59}N_5Zn$ requires 903.4886).

[5-(4-Aminophenyl)-10,15,20-tris(4-pentylphenyl)-21H,23H-porphinato]zinc 4. Mp 101–104 °C; λ_{\max} (CH_2Cl_2)/nm 425 ($\epsilon/dm^3 \text{ mol}^{-1} \text{ cm}^{-1}$ 100 000), 551 (35 400) and 592 (12 900); $\delta_H(CDCl_3)$ concentration-dependent, 9.11 (2H, d, *J* 7, β -pyrrolic H), 8.98 (2H, d, *J* 7, β -pyrrolic H), 8.45 (2H, d, *J* 7, β -pyrrolic H), 8.36 (2H, d, *J* 7, β -pyrrolic H), 8.30 (2H, d, *J* 7, 15-H_o), 7.64 (2H, d, *J* 7, 15-H_m), 7.86 (4H, d, *J* 7, 10- and 20-H_o), 7.08 (6H, m, 10- and 20-H_m and 5-H₂ and 5-H₆), 3.71 (2H, d, *J* 7, 5-H₃ and 5-H₅), 3.04 (2H, t, *J* 7, ArCH₂), 2.75 (4H, t, *J* 7, ArCH₂), 2.00 (2H, qn, *J* 7, CH₂), 1.73 (4H, qn, *J* 7, CH₂), 1.45 (2H, m, CH₂), 1.30 (4H, m, 2 \times CH₂), 1.11 (3H, t, *J* 7, CH₃), 0.93 (6H, t, *J* 7 Hz, CH₃), 0.35 (2H, s, NH₂); *m/z* (FAB) 903 (M^+ , $C_{59}H_{59}N_5Zn$ requires 903.4886).

Acknowledgements

We thank Pfizer and the EPSRC (AJG), the Spanish government (CR) and the Lister Institute (CAH) for financial support.

References

- 1 J. S. Lindsey, *New J. Chem.*, 1991, **15**, 153.
- 2 M. Fujita, J. Yazaki and K. Ogura, *J. Am. Chem. Soc.*, 1990, **112**, 5645.
- 3 M. Fujita, S. Nagao and K. Ogura, *J. Am. Chem. Soc.*, 1995, **117**, 1649.
- 4 S. C. Zimmerman and B. F. Duerr, *J. Org. Chem.*, 1992, **57**, 2215.
- 5 S. C. Zimmerman, F. W. Zeng, D. E. C. Reichert and S. V. Kolotuchin, *Science*, 1996, **271**, 1095.
- 6 D. P. Funeriu, J. M. Lehn, G. Baum and D. Fenske, *Chem. Eur. J.*, 1997, **3**, 99.
- 7 P. N. W. Baxter, J. M. Lehn, J. Fischer and M. T. Youinou, *Angew. Chem., Int. Ed. Engl.*, 1994, **33**, 2284.
- 8 N. Kimizuka, S. Fujikawa, H. Kuwahara, T. Kunitake, A. Marsh and J. M. Lehn, *J. Chem. Soc., Chem. Commun.*, 1995, 2103.
- 9 P. J. Stang, N. E. Persky and J. Manna, *J. Am. Chem. Soc.*, 1997, **119**, 4777.
- 10 J. Yang, J. L. Marendaz, S. J. Geib and A. D. Hamilton, *Tetrahedron Lett.*, 1994, **35**, 3665.
- 11 N. Branda, R. Wyler and J. Rebek, *Science*, 1994, **263**, 1267.
- 12 G. M. Whitesides, E. E. Simanek, J. P. Mathias, C. T. Seto, D. N. Chin, M. Mammen and D. M. Gordon, *Acc. Chem. Res.*, 1995, **28**, 37.
- 13 C. M. Drain, R. Fischer, E. G. Nolen and J. M. Lehn, *J. Chem. Soc., Chem. Commun.*, 1993, 243.
- 14 C. M. Drain and J. M. Lehn, *J. Chem. Soc., Chem. Commun.*, 1994, 2313.
- 15 H. L. Anderson, *Inorg. Chem.*, 1994, **33**, 972.
- 16 P. J. Stang, J. Fan and B. Olenyuk, *Chem. Commun.*, 1997, 1453.
- 17 C. A. Hunter and L. D. Sarson, *Angew. Chem., Int. Ed. Engl.*, 1994, **33**, 2313.
- 18 X. L. Chi, A. J. Guerin, R. A. Haycock, C. A. Hunter and L. D. Sarson, *J. Chem. Soc., Chem. Commun.*, 1995, 2567.
- 19 C. A. Hunter and R. K. Hyde, *Angew. Chem., Int. Ed. Engl.*, 1996, **35**, 1936.
- 20 J. K. M. Sanders, *Compr. Supramol. Chem.*, 1996, **9**, 131.
- 21 J. S. Lindsey and R. W. Wagner, *J. Org. Chem.*, 1989, **54**, 828.
- 22 J. S. Lindsey, K. A. Maccrum, J. S. Tyhonas and Y. Y. Chuang, *J. Org. Chem.*, 1994, **59**, 579.
- 23 X. L. Chi, A. J. Guerin, R. A. Haycock, C. A. Hunter and L. D. Sarson, *J. Chem. Soc., Chem. Commun.*, 1995, 2563.
- 24 R. J. Abraham and K. M. Smith, *J. Am. Chem. Soc.*, 1983, **105**, 5734.
- 25 K. M. Smith, F. W. Bobe, D. A. Goff and R. J. Abraham, *J. Am. Chem. Soc.*, 1986, **108**, 1111.
- 26 P. Leighton, J. A. Cowan, R. J. Abraham and J. K. M. Sanders, *J. Org. Chem.*, 1988, **53**, 733.
- 27 C. A. Hunter and M. J. Packer, submitted.
- 28 K. J. Cross and P. E. Wright, *J. Magn. Reson.*, 1985, **64**, 220.
- 29 F. Mohamadi, N. G. J. Richards, W. C. Guida, R. Liskamp, M. Lipton, C. Caufield, G. Chang, T. Hendrickson and W. C. Still, *J. Comput. Chem.*, 1990, **11**, 440.

Paper 8/07876I